

## Angle-resolved Auger spectrum of the N<sub>2</sub> molecule

A. Kivimäki,\* M. Neeb, B. Kempgens, H. M. Köppe, and A. M. Bradshaw  
*Fritz-Haber-Institut der Max-Planck-Gesellschaft, Faradayweg 4-6, 14195 Berlin, Germany*  
 (Received 25 October 1995; revised manuscript received 9 May 1996)

Angle-resolved Auger electron spectra of N<sub>2</sub> have been measured with good statistics at photon energies corresponding to the  $\pi^*$  resonance and the  $\sigma^*$  shape resonance, below and above the N 1s threshold, respectively. Angular anisotropy is observed in both cases, but disappears as expected far above threshold. Satellite Auger transitions also show some angular anisotropy close to the N 1s threshold. This is attributed to the creation and decay of conjugate shakeup initial states, which have non-ground-state symmetry. [S1050-2947(96)05809-X]

PACS number(s): 33.80.Eh, 33.60.Fy

### I. INTRODUCTION

In 1980 Dill *et al.* [1] predicted that Auger electron decay from molecular *K* hole states in aligned molecules should show anisotropic angular distribution patterns. Alignment occurs when primary excitation involves a transition into a bound or a continuum state of particular symmetry. Within the dipole approximation the angular distribution of Auger electrons from a cylindrically symmetric molecule can be written as

$$\frac{d\sigma(h\nu, \theta)}{d\Omega} = \frac{\sigma}{4\pi} [1 + \beta(h\nu)P_2(\cos\theta)] \quad (1)$$

assuming that randomly oriented molecules are probed with linearly polarized light.  $h\nu$  represents the photon energy and  $P_2(\cos\theta)$  is the second Legendre polynomial,  $\theta$  being the angle between the electric vector of the exciting radiation and the direction of observation. The experimentally observable angular anisotropy  $\beta$  is the product of two parameters:

$$\beta = \beta_m(h\nu)c_a, \quad (2)$$

where  $\beta_m$  describes the photon-energy-dependent molecular orientation with respect to the electric vector of the exciting radiation. Its value can range from  $-1$  to  $2$ .  $\beta_m = 0$  indicates no alignment of the molecule; i.e., no angular anisotropy is observed. The parameter  $c_a$  represents the intrinsic anisotropy of the Auger decay and is a constant for a given Auger transition. As an example, Dill *et al.* [1] calculated the molecular alignment parameter  $\beta_m$  in the  $\sigma^*$  resonances of CO and N<sub>2</sub> using the continuum multiple-scattering method. They obtained values exceeding 1 for both the C 1s (CO) and N 1s (N<sub>2</sub>) shape resonances, which would imply a considerable degree of molecular orientation. Later Lynch also reported calculated  $\beta_m$  values for these two molecules at the  $\sigma^*$  resonance [2]. Recently, Yagishita *et al.* [3] have shown that the molecular alignment can actually be determined directly from symmetry-resolved ion-yield absorption spectra.

Combined with such data, angle-resolved Auger electron spectra can therefore yield the intrinsic anisotropy parameter  $c_a$  of individual Auger lines.

Stimulated by the work of Dill *et al.* [1], the first attempts to measure angular anisotropy in molecular Auger spectra were performed on CO [4,5] and N<sub>2</sub> [6] but failed to reveal any conclusive effect. Later, however, Becker and co-workers were able to observe angular anisotropy in Auger decay following the C 1s  $\rightarrow \pi^*$  and C 1s  $\rightarrow \sigma^*$  excitations in CO by using higher electron energy resolution [7–9]. Because of the close similarity to CO, the effect is also expected to appear in N<sub>2</sub> [1] but its identification has obviously been hampered by more stringent experimental requirements. The nitrogen Auger lines have higher kinetic energies than those of carbon in CO, making time-of-flight spectrometers less suitable for their study. We have now measured the Auger spectra of N<sub>2</sub> at the  $\pi^*$  and  $\sigma^*$  resonances using an angle-resolving electrostatic electron spectrometer and high-intensity undulator radiation. These measurements indeed prove the existence of angular anisotropy in the N<sub>2</sub> Auger transitions from the aligned resonant states. As expected, the angular anisotropy disappears in the sudden limit. Such ‘‘normal’’ Auger transitions can, nevertheless, still show angular anisotropy if the decay of specifically oriented N<sub>2</sub> molecules is observed, as was recently done by Wood *et al.* [10] using the fragment ion–Auger electron coincidence method with electron impact excitation.

### II. EXPERIMENT

The Auger electron spectra of N<sub>2</sub> were measured on the X1B undulator beamline [11] at the 2.5-GeV electron storage ring of the National Synchrotron Light Source (NSLS), Brookhaven National Laboratory, using a cylindrical-mirror analyzer (CMA). The radiation is monochromatized with a Dragon-type spherical grating monochromator [12] and then passes along the symmetry axis of the CMA to intersect with target gas [13].

Only those electrons can enter the analyzer that are emitted in the reverse direction at the magic angle ( $\theta_m = 54.7^\circ$ ) with respect to the light propagation vector. Choosing the coordinate axes so that the photon beam is in the  $z$  direction and the major polarization vector ( $\mathbf{E}$ ) is oriented in the  $x$  direction, Eq. (1) can be expressed in the form [14]

\*Permanent address: Department of Physical Sciences, University of Oulu, 90570 Oulu, Finland.

$$\frac{d\sigma}{d\Omega} = \frac{\sigma}{4\pi} \left( 1 - \frac{1}{2}\beta \left[ P_2(\cos\theta_z) - \frac{3}{2}P(\cos^2\theta_x - \cos^2\theta_y) \right] \right), \quad (3)$$

where  $P$  is the degree of polarization and  $\theta_x, \theta_y, \theta_z$  denote the angles between the corresponding axes and the direction of observation. In the present case  $\theta_z = \theta_m$  for which the Legendre polynomial  $P_2$  has the value 0. The remaining terms can be organized to give

$$\left( \frac{d\sigma}{d\Omega} \right)_{\theta_z = \theta_m} = \frac{\sigma}{4\pi} \left[ 1 + \frac{1}{2}\beta P \cos 2\varphi \right], \quad (4)$$

where  $\varphi$  is the angle between the  $x$  axis and the projection of the direction of observation on the  $x$ - $y$  plane. A circular microchannel plate detector, divided into eight segments each spanning  $45^\circ$ , is situated in this plane in front of the focal point of the analyzer. The dependence of intensity on  $\beta$  and  $P$  can be calculated exactly for each detector segment by integrating Eq. (4) over the appropriate values of the angle  $\varphi$  [15]. Experimental angular anisotropies can be determined in a straightforward way from the intensities of the segments bisected by the  $x$  and  $y$  axes:

$$P\beta = \frac{\pi}{\sqrt{2}} \frac{I_x - I_y}{I_x + I_y}, \quad (5)$$

provided that the degree of polarization  $P$  of the exciting radiation is known. Note that although the electrons are collected in segments that span  $45^\circ$ , the determination of the  $\beta$  values is not affected, as the integrations over  $\varphi$  show. The added intensity of all the segments, on the other hand, is directly proportional to the cross section  $\sigma$ . This arrangement thus allows angle-resolved electron spectra to be measured at the same time as the angle-independent intensity without the need to physically move any components.

All spectra shown in this paper were measured using the same two detector segments. Apart from normalization to light intensity and target gas pressure, no scaling or any other data manipulation was performed. The degree of polarization  $P$  of the exciting radiation was determined to be 81–82% in the photon energy range 400–480 eV by measuring the angle-resolved Ne  $2s$  photoelectron line, the asymmetry parameter of which is 2. The photon bandwidth was set to about 0.4 eV at the  $\pi^*$  resonance. For the measurements above the N  $1s$  threshold, the slits were fully opened and the photon energy resolution was 2 eV or higher. The electron spectrometer was operated in the constant pass energy mode with retardation to 80 eV, resulting in kinetic energy resolution of 0.6–0.7 eV. The kinetic energy scale was calibrated using the N<sub>2</sub>  $KLL$  Auger spectrum of Siegbahn *et al.* [16].

### III. RESULTS AND DISCUSSION

#### A. $\pi^*$ resonance

The N  $1s$  absorption spectrum of N<sub>2</sub> [17] is dominated by the intense  $1s \rightarrow \pi^*$  excitation, located 9 eV below the ionization threshold at 409.9 eV. The  $\pi^*$  excited state decays predominantly via Auger-like transitions (so-called resonant Auger), where the excited electron actively takes part in the

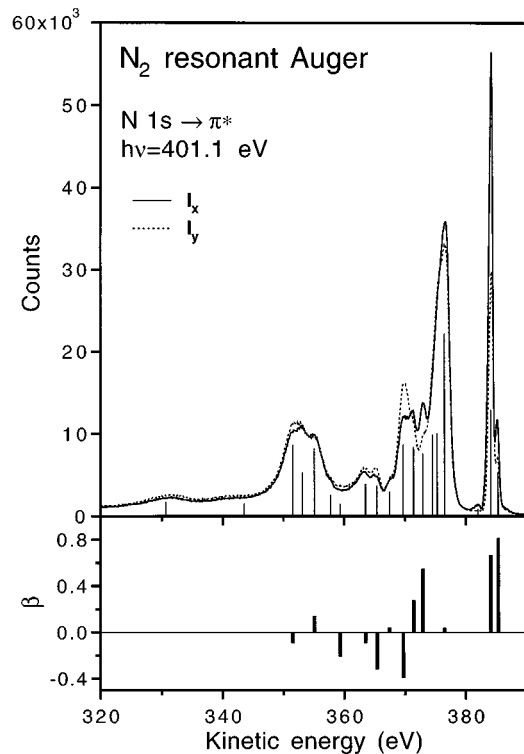


FIG. 1. The angle-resolved resonant Auger spectrum of N<sub>2</sub> measured at the  $\pi^*$  resonance ( $h\nu = 401.1$  eV). Intensity parallel to the electric vector of the exciting radiation ( $I_x$ ) is plotted with a solid line and perpendicular ( $I_y$ ) with a dotted line. The thin lines under the intensity curves denote fitted peak positions while the thicker bars in the lower part give the asymmetry parameter  $\beta$  derived for these transitions. Most  $\pi^*$  resonant Auger lines show clear angular anisotropy.

decay process (participator decay) or merely acts as a “passive” spectator while one valence electron fills the core hole and another one is ejected (spectator decay). Thus, the initial states of the resonant Auger transitions are neutral and the final states are singly ionized, in contrast to the normal Auger decay where the initial and final states are singly and doubly ionized, respectively. Figure 1 shows angle-resolved  $\pi^*$  resonant Auger spectra of N<sub>2</sub>, recorded with the mean photon energy of 401.1 eV. The lines around 385-eV kinetic energy are caused by participator transitions, as discussed earlier by Eberhardt *et al.* [18], and correspond to the single hole final states  $1\pi_u^{-1}$  and  $3\sigma_g^{-1}$ . The peaks below 380 eV mostly arise from spectator transitions where the  $1\pi_g$  orbital is also occupied in the final state.

It is quite clear from Fig. 1 that most of the resonant Auger lines show some degree of angular anisotropy. To obtain more quantitative results a fit procedure was adopted in which the position and width of each transition were assumed to be the same in the two spectra and the intensities were allowed to vary independently. The vertical lines under the spectra show the locations of the fitted peaks, but do not represent real intensities; they are simply shown as a guide to the eye. The asymmetry parameters derived are displayed as bars in the lower part of Fig. 1. The low kinetic energy transitions up to 370 eV possess mostly negative  $\beta$  values, as in the case of the C  $1s \rightarrow \pi^*$  resonant Auger spectrum of the isoelectronic CO molecule [8]. However, the most intense

lines have positive angular anisotropies. Integration over the two curves yields a value of  $0.04(\pm 0.03)$  for the average  $\beta$ . The error limits given indicate the contribution due to the (non)scaling of the segment intensities. This error in  $\beta$  also appears for individual lines for which there is an additional uncertainty due to fitting. The latter can be as high as  $\pm 0.1$  for badly resolved features but is negligible for the two participator transitions.

The allowed values of the intrinsic Auger anisotropy parameter  $c_a$  are given by the condition  $-1 \leq \beta_m c_a \leq 2$  [1]. After a  $1s \rightarrow \pi^*$  excitation, a diatomic molecule preferentially lies with its axis perpendicular to the electric vector of the linearly polarized exciting radiation, which corresponds to the molecular orientation parameter  $\beta_m = -1$  [1]. Thus, for the Auger decay from pure  $\pi^*$  excited states, the  $c_a$  values are restricted to the range  $-2$  to  $1$ . The experimentally determined molecular orientation  $\beta_m$  at the  $\pi^*$  resonance of N<sub>2</sub> is  $-0.9$  [3,19,20]. Using this experimental  $\beta_m$  and the  $\beta$  values of  $0.67(\pm 0.04)$  and  $0.81(\pm 0.04)$  from Fig. 1, Eq. (2) gives  $c_a = -0.74$  and  $-0.90$  for the two intense participator transitions to the final states  $1\pi_u^{-1}$  and  $3\sigma_g^{-1}$ , respectively. Direct photoemission also yields electrons at the same kinetic energies but here it accounts for less than 2% of the total intensity of the  $1\pi_u^{-1}$  and  $3\sigma_g^{-1}$  lines and thus does not appreciably alter the angular distribution. The spectator resonant Auger transitions have the intrinsic anisotropy parameters  $c_a$  between  $-0.6$  and  $0.4$ . Thus, our results support the view that Eq. (2) is also valid for resonant Auger processes, even though it was derived for the sudden-limit regime neglecting the interference effects that have been shown to occur in N<sub>2</sub> [21].

### B. $\sigma^*$ resonance

The photoabsorption cross section of N<sub>2</sub> is enhanced by the presence of the  $\sigma_u$  shape resonance [22] in the region 5–15 eV above the N  $1s$  ionization threshold. Consequently, in this energy range core-ionized molecules are also expected to show a net alignment, which should affect the angular distribution of emitted Auger electrons. Our angle-resolved spectrum, displayed in Fig. 2, was measured at 421.6-eV photon energy, i.e., slightly above the maximum of the shape resonance [23]. It can easily be seen that some Auger lines in the kinetic energy range 357–367 eV show the predicted angular anisotropy. Similarly, the satellite Auger structure at 375 eV [24] also seems to be anisotropic in its angular distribution; its behavior will be discussed in more detail in the next section. The feature in the spectrum at 383.5-eV kinetic energy (furthest right) that shows the largest effect ( $\beta \approx 1.5$ ) is not caused by Auger decay but by direct  $2\sigma_g^{-1}$  photoionization.

In contrast to the  $\pi^*$  spectrum, the  $\sigma^*$  resonant Auger spectrum is characterized by structures that are also present in the “normal” Auger spectrum measured far above threshold [14,25–27]. The  $\beta$  values determined from the fit are shown as bars in the lower part of Fig. 2 and are also given in Table I. Their absolute values are slightly uncertain due to the complexity of the spectral features, but the trends are clear. The Auger line at 360.4-eV kinetic energy shows a negative  $\beta$  value. Ågren [28] has assigned this peak to a  $1\Pi_g$  symmetry final state with the leading electron configu-

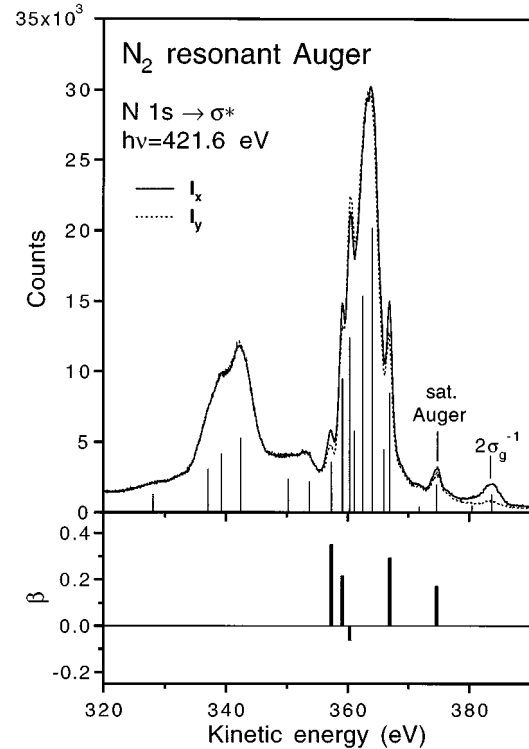


FIG. 2. The angle-resolved Auger spectrum of N<sub>2</sub> measured at the  $\sigma^*$  resonance with photon energy 421.6 eV. For details, see the caption of Fig. 1. Angular anisotropy is observed for some Auger lines in the kinetic energy range 357–367 eV.

ration  $2\sigma_u^{-1}1\pi_u^3\psi$ . In the dominant Auger group three other lines, all of  $\Sigma$  final-state symmetry, have positive  $\beta$  values. We refrain, however, from drawing a correlation between the  $\Pi$  or  $\Sigma$  symmetry of the final state and the sign of the asymmetry parameter, because the situation in the CO molecule appears to be partly contradictory [8,29]. The molecular orientation is in principle described by  $\beta_m = 2$  for a  $1s\sigma \rightarrow \sigma^*$  transition but the additional, almost constant contribution from  $\pi$ -type absorption in the continuum [23] lowers this value. Using the experimental result of  $0.8$  for  $\beta_m$  at  $h\nu = 421.6$  eV [3,19], the intrinsic anisotropies  $c_a$  of the Auger lines are found to extend from  $-0.1$  to  $0.4$ . The mean angular asymmetry for the N<sub>2</sub> Auger transitions at 421.6-eV photon energy equals zero within the error bars ( $\beta = 0.02 \pm 0.03$ ) when the integration is carried out up to 370 eV. This demonstrates the need for high resolution in order to observe the subtle angular distribution effects in molecular  $K$ -shell Auger decay.

TABLE I. The observed  $\beta$  values for the N<sub>2</sub> Auger transitions at  $h\nu = 421.6$  eV. The assignments are taken from Refs. [14,25,26,28].

Kinetic energy (eV)	Transition	$\beta$
357.3	$1s^{-1} \rightarrow 2\sigma_u^{-2}(1\Sigma_g)$	$0.35(\pm 0.08)$
359.1	$1s^{-1} \rightarrow 2\sigma_u^1 3\sigma_g^1(1\Sigma_u)$	$0.22(\pm 0.05)$
360.4	$1s^{-1} \rightarrow 2\sigma_u^1 1\pi_u^2(1\Pi_g)$	$-0.06(\pm 0.08)$
366.9	$1s^{-1} \rightarrow 3\sigma_g^{-2}(1\Sigma_g)$	$0.30(\pm 0.08)$
$\sim 375$	Satellite Auger	$0.17(\pm 0.08)$

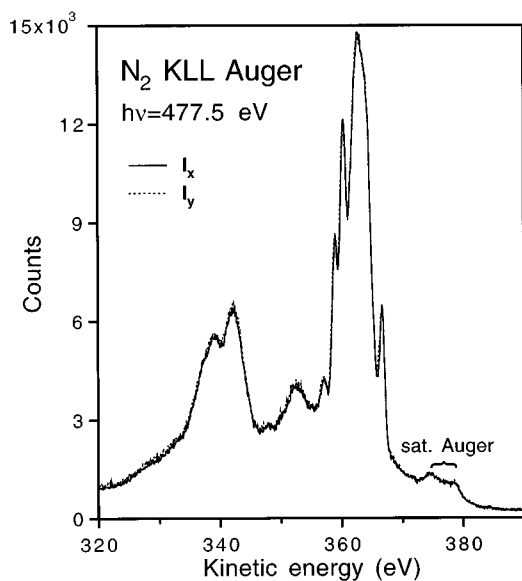


FIG. 3. The angle-resolved intensity curves for the normal Auger spectrum of  $N_2$  measured at  $h\nu=477.5$  eV. No conclusive angular anisotropy is observed.

For comparison, we present in Fig. 3 the normal Auger spectrum of  $N_2$  measured at 477.5-eV photon energy, i.e., far above the  $N\ 1s$  threshold. The two curves are almost identical; only in the low kinetic energy part is the intensity perpendicular to the electric vector ( $I_y$ ) on average very slightly higher. This effect might be caused by nonhomogeneities in the electric field of the analyzer, although asymmetric electron emission due to the manifold of ionized states far above threshold cannot be excluded. If it is indeed caused by instrumental imperfections, the potential error for the  $\beta$  determination is still very small ( $\pm 0.03$ ) and any correction procedures for the detection sensitivity are redundant. (The scaling error in the present studies has been estimated from this spectrum assuming that the intensities of the two segments should be equal far above threshold.) Note also that the spectra shown in Figs. 1–3 were measured immediately after each other.

### C. Satellite Auger features

In a previous paper [24] we studied the intensity behavior of the satellite Auger structures of the  $N_2$  molecule located at 370–380-eV kinetic energies. The 375-eV Auger peak was correlated mainly with participator decay from the ‘triplet-coupled’  $1\pi_u^{-1}1\pi_g^1(3\Sigma_u)1s^{-1}$  shakeup state. Close to the satellite threshold, the corresponding photoelectron line increases in intensity due to the conjugate part of the transition moment and is accompanied by pure conjugate shakeup satellites. The latter have non-ground-state symmetries [30] and give rise to aligned molecules, in contrast to the normal shakeup satellites. Since the pure conjugate shakeup lines lie close to the triplet-coupled  $\pi\pi^*$  satellite in the photoelectron spectrum, the participator decay from these states is also expected to contribute to the 375-eV Auger peak. This can be clarified by a study of possible angular effects, which, in turn, requires better statistics than was available in Ref. [24]. The satellite Auger spectra have therefore been remeasured in the photon energy range 423–443

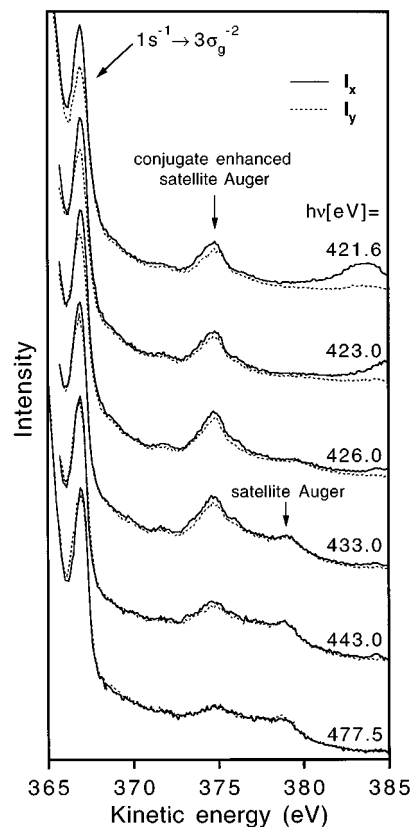


FIG. 4. The satellite Auger part of the  $N_2$  *KLL* Auger spectrum measured with angular resolution. The feature moving to higher kinetic energies in the uppermost spectra is the  $2\sigma_g$  photoelectron line and the most intense structure at 366.9-eV kinetic energy is the  $1s^{-1}\rightarrow 3\sigma_g^{-2}$  diagram Auger line. Note the changing angular anisotropy of the conjugate-enhanced satellite Auger peak at 375-eV kinetic energy.

eV; the results are shown in Fig. 4, along with the relevant portions of the spectra from Figs. 2 and 3.

The satellite Auger peak at 375-eV kinetic energy indeed shows angular anisotropy at close-to-threshold photon energies and the corresponding asymmetry parameter varies as the photon energy is changed. The other satellite Auger peak at 379-eV kinetic energy, arising from the normal singlet-coupled  $\pi\pi^*$  shakeup state above its threshold at 426.2 eV, [24,27] displays no angular anisotropy outside the scatter of the data. Since this peak lies between the 375-eV satellite Auger feature and the  $2\sigma_g$  photoelectron line, the tail of the latter can also be excluded as the origin of the changing angular anisotropy. From the fit,  $\beta$  of the satellite Auger line at 375 eV is  $0.17(\pm 0.08)$  for the three lowest photon energies in Fig. 4, decreases ( $\beta=0.07$  at 443 eV) and then goes to zero far above threshold. This behavior agrees well with the emergence and disappearance of the pure conjugate shakeup satellite lines in the photoelectron spectrum [24]. Based on the different behavior of the two satellite Auger peaks, we therefore attribute the observed behavior in the angular anisotropy of the satellite Auger emission to the existence of pure conjugate shakeup satellites. We also conclude that some Auger transitions from the pure conjugate shakeup initial states have quite large  $\beta$  values since a net angular anisotropy is still observed at 375-eV kinetic energy even though the predominant decay comes from the triplet-

coupled  $\pi\pi^*$  shakeup initial states of ground-state symmetry.

A different interpretation for the angular asymmetry was originally given by Becker and co-workers [8] for the satellite Auger peaks in CO. They related the angular anisotropy to the shape resonances in the conjugate shakeup satellite cross sections. More recently, however, the same authors have reinvestigated the CO satellite Auger spectrum [5,9], this time attributing the angular anisotropy to the decay of the aligned ionic states. In the case of N<sub>2</sub>, it is clear that the shape resonance is not the main origin of the observed angular anisotropy. If it were to play a significant role in N<sub>2</sub>, then not only the 375-eV satellite Auger peak but also the one at 379 eV should show angular anisotropy. Moreover, the angular anisotropy of the 375-eV satellite Auger peak already seems to be strong immediately at threshold and does not show any maximum in the shape resonance region.

#### IV. CONCLUSIONS

We have measured the angle-resolved Auger spectrum of the N<sub>2</sub> molecule at the  $\pi^*$  and  $\sigma^*$  resonances as well as far

above the N 1s ionization threshold. As predicted by Dill *et al.* [1], the Auger spectrum at the  $\sigma^*$  resonance shows angular anisotropy. The effect is only observed for certain Auger lines, whereas at the  $\pi^*$  resonance angular anisotropy is observed throughout the spectrum. In both cases the mean angular anisotropy is almost zero, which explains why the effect could not be verified with low electron energy resolution [6]. The satellite Auger feature at 375-eV kinetic energy also displays angular anisotropy, in contrast to the satellite Auger peak at 379 eV. In this case we suggest that the effect derives from decay of pure conjugate shakeup initial states. Far above threshold both the normal and satellite Auger emission becomes isotropic.

#### ACKNOWLEDGMENTS

We acknowledge financial support from the German Federal Ministry of Science, Education, Research and Technology (BMBF) under Contract No. 05 5EBFXB 2. The National Synchrotron Light Source at Brookhaven National Laboratory is supported by the U.S. Department of Energy under Contract No. DE-AC02-76CH00016.

- 
- [1] D. Dill, J. R. Swanson, S. Wallace, and J. L. Dehmer, *Phys. Rev. Lett.* **45**, 1393 (1980).
- [2] D. L. Lynch, *Phys. Rev. A* **43**, 5176 (1991).
- [3] A. Yagishita, H. Maezawa, M. Ukai, and E. Shigemasa, *Phys. Rev. Lett.* **62**, 36 (1989).
- [4] C. M. Truesdale, S. H. Southworth, P. H. Kobrin, U. Becker, D. W. Lindle, H. G. Kerkhoff, and D. A. Shirley, *Phys. Rev. Lett.* **50**, 1265 (1983).
- [5] C. M. Truesdale, D. W. Lindle, P. H. Kobrin, U. Becker, H. G. Kerkhoff, P. H. Heimann, T. A. Ferrett, and D. A. Shirley, *J. Chem. Phys.* **80**, 2319 (1984).
- [6] D. W. Lindle, C. M. Truesdale, P. H. Kobrin, T. A. Ferrett, P. H. Heimann, U. Becker, H. G. Kerkhoff, and D. A. Shirley, *J. Chem. Phys.* **81**, 5375 (1984).
- [7] U. Becker, R. Hölzel, H. G. Kerkhoff, B. Langer, D. Szostak, and R. Wehlitz, *Phys. Rev. Lett.* **56**, 1455 (1986).
- [8] O. Hemmers, F. Heiser, J. Eiben, R. Wehlitz, and U. Becker, *Phys. Rev. Lett.* **71**, 987 (1993).
- [9] O. Hemmers, S. B. Whitfield, N. Berrah, B. Langer, R. Wehlitz, and U. Becker, *J. Phys. B* **28**, L693 (1995).
- [10] R. M. Wood, Q. Zheng, M. A. Mangan, and A. K. Edwards, *Nucl. Instrum. Methods B* **99**, 39 (1995).
- [11] K. J. Randall, J. Feldhaus, W. Erlebach, A. M. Bradshaw, W. Eberhardt, Z. Xu, Y. Ma, and P. D. Johnson, *Rev. Sci. Instrum.* **63**, 1367 (1992).
- [12] C. T. Chen, *Nucl. Instrum. Methods A* **256**, 595 (1987).
- [13] J. Feldhaus, W. Erlebach, A. L. D. Kilcoyne, K. J. Randall, and M. Schmidbauer, *Rev. Sci. Instrum.* **63**, 1454 (1992).
- [14] S. T. Manson and A. F. Starace, *Rev. Mod. Phys.* **54**, 389 (1982).
- [15] M. Schmidbauer, Doctoral thesis, Technische Universität Berlin, 1992 (unpublished).
- [16] K. Siegbahn, C. Nordling, G. Johansson, J. Hedman, P. F. Hedén, K. Hamrin, U. Gelius, T. Bergmark, L. O. Werme, R. Manne, and Y. Baer, *ESCA Applied to Free Molecules* (North-Holland, Amsterdam, 1969).
- [17] C. T. Chen, Y. Ma, and F. Sette, *Phys. Rev. A* **40**, 6737 (1989).
- [18] W. Eberhardt, E. W. Plummer, I.-W. Lyo, R. Murphy, R. Carr, and W. K. Ford, *J. Phys. (Paris), Colloq. Suppl.* **12** **48**, C9-679 (1987). See also W. Eberhardt, J.-E. Rubensson, K. J. Randall, J. Feldhaus, A. L. D. Kilcoyne, A. M. Bradshaw, Z. Xu, P. D. Johnson, and Y. Ma, *Phys. Scr.* **T41**, 143 (1992).
- [19] E. Shigemasa, K. Ueda, Y. Sato, T. Hayaishi, H. Maezawa, T. Sasaki, and A. Yagishita, *Phys. Scr.* **41**, 63 (1990).
- [20] K. Lee, D. Y. Kim, C. I. Ma, D. A. Lapiano-Smith, and D. M. Hanson, *J. Chem. Phys.* **93**, 7936 (1990).
- [21] J.-E. Rubensson, M. Neeb, M. Biermann, Z. Xu, and W. Eberhardt, *J. Chem. Phys.* **99**, 1633 (1993).
- [22] J. L. Dehmer and D. Dill, *Phys. Rev. Lett.* **35**, 213 (1975).
- [23] E. Shigemasa, K. Ueda, Y. Sato, T. Sasaki, and A. Yagishita, *Phys. Rev. A* **45**, 2915 (1992).
- [24] M. Neeb, A. Kivimäki, B. Kempgens, H. M. Köppe, A. M. Bradshaw, and J. Feldhaus, *Phys. Rev. A* **52**, 1224 (1995).
- [25] D. Stalherm, B. Cleff, H. Hillig, and W. Melhorn, *Z. Naturforsch. A* **24**, 1728 (1969).
- [26] W. E. Moddeman, T. A. Carlson, M. O. Krause, B. P. Pullen, W. E. Bull, and G. K. Schweitzer, *J. Chem. Phys.* **55**, 2317 (1971).
- [27] S. Svensson, A. Naves de Brito, M. Keane, N. Correia, L. Karlsson, C.-M. Liegener, and H. Ågren, *J. Phys. B* **25**, 135 (1992).
- [28] H. Ågren, *J. Chem. Phys.* **75**, 1267 (1981).
- [29] L. S. Cederbaum, P. Campos, F. Tarantelli, and A. Sgamellotti, *J. Chem. Phys.* **95**, 6634 (1991).
- [30] G. Angonoa, O. Walter, and J. Schirmer, *J. Chem. Phys.* **87**, 6789 (1987).